



ARTICLE

Striato-cortical tracts predict 12-h abstinence-induced lapse in smokers

Kai Yuan^{1,2,3,4,5}, Meng Zhao^{1,3}, Dahua Yu³, Peter Manza², Nora D. Volkow^{2,6}, Gene-Jack Wang² and Jie Tian^{1,3,7}

Striatal circuit dysfunction is implicated in smoking behaviors and lapses during abstinence attempts. However, little is known about whether the structural connectivity of striatal tracts can be used to predict abstinence-induced craving and lapses. The tract strengths of striatal circuits were compared in 53 male nicotine-dependent cigarette smokers and 58 matched nonsmokers, using seed-based classification by diffusion tensor imaging (DTI) probabilistic tractography with 10 a priori target masks. A 12-h abstinence procedure was then employed, after which 31 individuals abstained and 22 lapsed. Linear regression and binary logistic regression was conducted to test whether the tract strength of frontostriatal circuits was associated with craving changes in abstainers and predicted lapse in smokers. Compared with nonsmokers, in the left hemisphere, smokers showed weaker tract strength in striatum-medial orbitofrontal cortex (mOFC), striatum-ventral lateral prefrontal cortex (vlPFC), striatum-inferior frontal gyrus (IFG) and striatum-posterior cingulate cortex (PCC) (Bonferroni corrected, $p < 0.05/20 = 0.0025$). In abstainers, the abstinence-induced increases in craving were associated with the tract strength of the left striatum-mOFC and striatum-vlPFC. The tract strength of left striatum-dorsolateral PFC (dlPFC) predicted lapse in smokers with an accuracy of 68.3%. These results provide system-level insights into the weaker tract strength of frontostriatal circuits in male smokers and their potential roles as neuroimaging markers for abstinence-induced craving and risk of lapse. Future studies in female smokers are needed to determine if this generalizes across genders.

Neuropsychopharmacology (2018) 43:2452–2458; <https://doi.org/10.1038/s41386-018-0182-x>

INTRODUCTION

Like most drugs of abuse, cigarette smoking exerts its initial reinforcing effects by activating reward circuits and releasing dopamine (DA) in the striatum [1–3]. Though initially smoking is largely a voluntary behavior, continued smoking triggers neuroplasticity and conditioning to smoking cues that automatize the behavior and impair self-regulation [4, 5]. A network of interacting brain regions and associated circuits has been shown to mediate smoking behaviors, including striatum, ventral tegmental area, amygdala/hippocampus, anterior cingulate cortex (ACC), dorsolateral prefrontal cortex (dlPFC), inferior frontal gyrus (IFG), ventral lateral PFC (vlPFC) and medial orbitofrontal cortex (mOFC) [6–8].

Recently, striatal functional interactions with mOFC and dlPFC during resting state [4, 9] and during smoking cue reactivity tasks [5, 10] were shown to be associated with smoking behaviors. Moreover, the structural connectivity of striatal tracts facilitates brain function and predicts decision making, cognitive control and personality [11, 12]. Although regional structural abnormalities [13, 14] and disrupted topological organization within frontostriatal white matter (WM) networks [15] have been observed in smokers, it is less known how system-level structural connections of striatal tracts are implicated in smoking behaviors.

Craving is a prominent feature of cigarette smoking [3, 16]. For most smokers, the vast majority of quit attempts are accompanied by increased craving and intermittent lapse within a period as short as 12–24 h [17]. In fact, approximately 85–95% of lapsed smokers ultimately relapse [18]. Neuroimaging markers of abstinence-induced smoking craving and of lapse would be very valuable for monitoring and tailoring treatment intervention for smoking cessation.

Data on striatal circuit function have shown their potential to predict relapse in smokers [19–21]. For instance, blunted brain responses of dorsal striatum and medial/dorsolateral prefrontal cortex (mPFC and dlPFC) to pleasant vs. cigarette-related stimuli predict relapse in smokers [21]. Further, brain responses in the ventromedial PFC to graphic warning labels, relative to a visual control image, predicted relapse in treatment-seeking nicotine-dependent smokers [19]. However, functional magnetic resonance imaging (MRI) cannot identify the structural connections between those circuits. In contrast, diffusion tensor imaging (DTI) tractography provides a measure of structural connectivity [5]. To our knowledge, the extent to which the structural connectivity of striatal tracts can predict lapse in smokers has not been investigated.

¹School of Life Science and Technology, Xidian University, Xi'an, Shaanxi 710071, People's Republic of China; ²National Institute on Alcoholism and Alcohol Abuse, National Institutes of Health, Bethesda, MD 20892, USA; ³Engineering Research Center of Molecular and Neuro Imaging Ministry of Education, Xi'an Shaanxi, 710071, People's Republic of China; ⁴Inner Mongolia Key Laboratory of Pattern Recognition and Intelligent Image Processing, School of Information Engineering, Inner Mongolia University of Science and Technology, Baotou, Inner Mongolia 014010, People's Republic of China; ⁵Guangxi Key Laboratory of Multi-Source Information Mining and Security, Guangxi Normal University, Guilin 541001, People's Republic of China; ⁶National Institute on Drug Abuse, National Institutes of Health, Bethesda, MD 20892, USA and ⁷Institute of Automation, Chinese Academy of Sciences, Beijing 100190, People's Republic of China
Correspondence: Kai Yuan (kyuan@xidian.edu.cn)

Received: 7 May 2018 Revised: 6 August 2018 Accepted: 7 August 2018
Published online: 15 August 2018

Table 1 Demographic characteristics of smokers in the satiated condition and of nonsmokers

Items	Smokers (n = 53)	Nonsmokers (n = 58)	t	P value
Age (years)	20.98 ± 1.69	20.69 ± 1.50	0.96	0.34
Education (years)	14.02 ± 1.20	13.78 ± 1.45	0.96	0.34
SAS	33.78 ± 6.43	30.31 ± 5.81	2.98	0.004
SDS	35.51 ± 7.38	32.36 ± 7.10	2.29	0.024
CO (ppm)	11.62 ± 1.71	1.67 ± 0.63	39.89 ^a	<0.001
Cigarettes per day (CPD)	14.62 ± 5.75	–	–	–
Onset age (years)	15.36 ± 2.39	–	–	–
Years of smoking	4.17 ± 1.85	–	–	–
Pack-years	3.10 ± 2.0	–	–	–
FTND	4.81 ± 1.78	–	–	–
QSU	24.6 ± 8.5	–	–	–

Values are mean ± SD

SAS Self-Rating Anxiety Scale, SDS Self-Rating Depression Scale, CO carbon monoxide, Pack-years smoking years × daily consumption/20, FTND Fagerström Test for Nicotine Dependence, QSU Questionnaire on Smoking Urges

^aNot equal variance

Bold values indicate a statistically significant difference with a p-value less than 0.05.

In the current study, we used seed-based classification with DTI probabilistic tractography to calculate the tract strength of the striatum to 10 a priori target masks (mOFC, dIPFC, vIPFC, IFG, posterior cingulate cortex (PCC), ACC, dorsal ACC (dACC), supplementary motor area (SMA), hippocampus and amygdala) according to previous studies [12, 22]. In 111 participants (53 male nicotine-dependent cigarette smokers and 58 matched nonsmokers), we compared the different tract strengths of the striatal centric circuits between two groups. We then separated the smokers into abstainers and lapsers using a 12-h smoking abstinence procedure. Then, among abstainers, we investigated whether the strength of specific striatal tracts in the satiated condition were associated with the percentage changes of smoking craving between the satiated and the abstinence conditions. Finally, in the whole cohort of smokers, binary logistic regression was used to verify whether specific striatal tract strength in the satiated condition could predict a smoking lapse induced by 12-h abstinence.

MATERIALS AND METHODS

Experimental design

Participants. We enrolled 53 male nicotine-dependent cigarette smokers (Diagnostic and Statistical Manual of Mental Disorders, 4th Edition (DSM-IV)) (age: 20.98 ± 1.69 years) and 58 age-, education- and gender-matched nonsmokers (age: 20.69 ± 1.50 years) from local universities. All smokers had no history of attempting to quit or of smoking abstinence in the past 6 months. The Fagerström Test for Nicotine Dependence (FTND) and pack-years of smoking were collected in smokers. Subjective craving was assessed using the brief 10-item form of the questionnaire for smoking urges. Nonsmokers were defined as those who had never smoked in their lifetime. Expiratory carbon monoxide (CO) levels of all participants were measured using the Smokerlyzer System (Bedfont Scientific, Ltd, Rochester, UK). CO level in expired air was verified as ≥10 parts per million (ppm) in smokers and ≤3 ppm in nonsmokers. All of the participants were right-handed as measured by the Edinburgh Handedness Inventory. The self-rating anxiety scale and self-rating depression scale were also collected for both groups.

Exclusion criteria for both groups were: (1) any physical illness according to clinical evaluations and medical records; (2) any Axis I psychiatric disorder as assessed with the structured clinical interview for DSM-IV; (3) urine test demonstrating current substance use (opioids and cocaine) other than nicotine dependence; (4) alcohol use disorder as measured by the Alcohol Use Disorders Identification Test (AUDIT); and (5) current use of any medications that could affect cognitive function. The demographic characteristics of participants are shown in Table 1.

The 12-h abstinence procedure in smokers. We instructed participants to have a good night's sleep and not to drink alcohol or coffee 48 h before the study days. In the first test day (satiated condition), smokers were asked to smoke one of their own brand cigarettes about 30 min before the recording of self-reports of craving. After 2–3 days, in the second test day (abstinence condition), smokers were not allowed to smoke between 10:00 pm and 10:00 am. Smokers were then separated into abstainers and lapsers based on whether they smoked in the 12-h period (10:00 pm to 10:00 am) prior to the MRI scanning procedure. Abstinence was confirmed by expired CO ≤8 ppm using the Smokerlyzer system (Bedfont Scientific Ltd., Rochester, UK) and self-report. Craving, anxiety and depression were collected in the abstinence condition to assess the changes from the satiated conditions.

MRI data acquisition

The experiment was carried out on a 3T Philips scanner (Achieva; Philips Medical Systems, Best, The Netherlands) at the First Affiliated Hospital of Baotou Medical College, Inner Mongolia University of Science and Technology, Baotou, China. For each smoker, MRI images were collected in the satiated condition, i.e., they smoked a cigarette about 40 min preceding the scan (average duration of abstinence before scan: 42.6 ± 18.2 min). Prior to the MRI scanning, subjects were instructed to refrain from alcohol and other drugs (including caffeine) consumption for the prior 48 h, which was confirmed with a urine drug screen and a breath test for alcohol. The scanning session started between 10:00 and 10:15 am. The three-dimensional (3D) T1-weighted images were acquired using a magnetization prepared rapid acquisition gradient echo (MPRAGE) pulse sequence with a voxel size of 1 × 1 × 1 mm³ (repetition time (TR) = 8.4 ms; echo time (TE) = 3.8 ms; data matrix = 240 × 240; slices = 176; field of view (FOV) = 240 × 240 mm²). DTI data were collected with a single-shot echo-planar imaging sequence (68 continuous axial slices with a slice thickness of 2 mm, TR = 6800 ms, TE = 70 ms, data matrix = 120 × 120, FOV = 240 × 240 mm²). To improve the signal-to-noise ratio, 2 repeat of the 32 non-collinear directions (b = 1000 s/mm²) were applied with 3 acquisitions without diffusion weighting (b = 0 s/mm²). The parallel acceleration factor (SENSE) was 2. The B0 field map was collected via a 3D interleaved dual echo gradient echo pulse sequence, with the following parameters: matrix size = 240 × 240, FOV = 240 × 240, TR = 10 ms, TE1 = 2.25 ms, TE2 = 3.25 ms. The same scanning parameters were used when acquiring the T1 and DTI data of nonsmokers.

Striatum structural connectivity analysis

Striatum seed and the target brain regions. The striatum seed was obtained from the combination of regions in the Harvard-subcortical structural atlas (caudate, putamen and nucleus accumbens (NAC); <https://fsl.fmrib.ox.ac.uk/fsl/fslwiki/Atlases>). To assess connectivity with extrastriatal regions, we used a set of 10 a priori masks defined in previous studies [12, 22]. These masks were defined based on one or a combination of several regions from standard automated anatomical labeling (AAL) maps: ACC (32), dACC (34), dIPFC (4, 8), PCC (68), IFG (triangular part IFG: 14), mOFC (28, 6, 26), vIPFC (10, 16), hippocampus (38), amygdala (42) and SMA (20) (Fig. 1a). All these regions of interests (striatum and

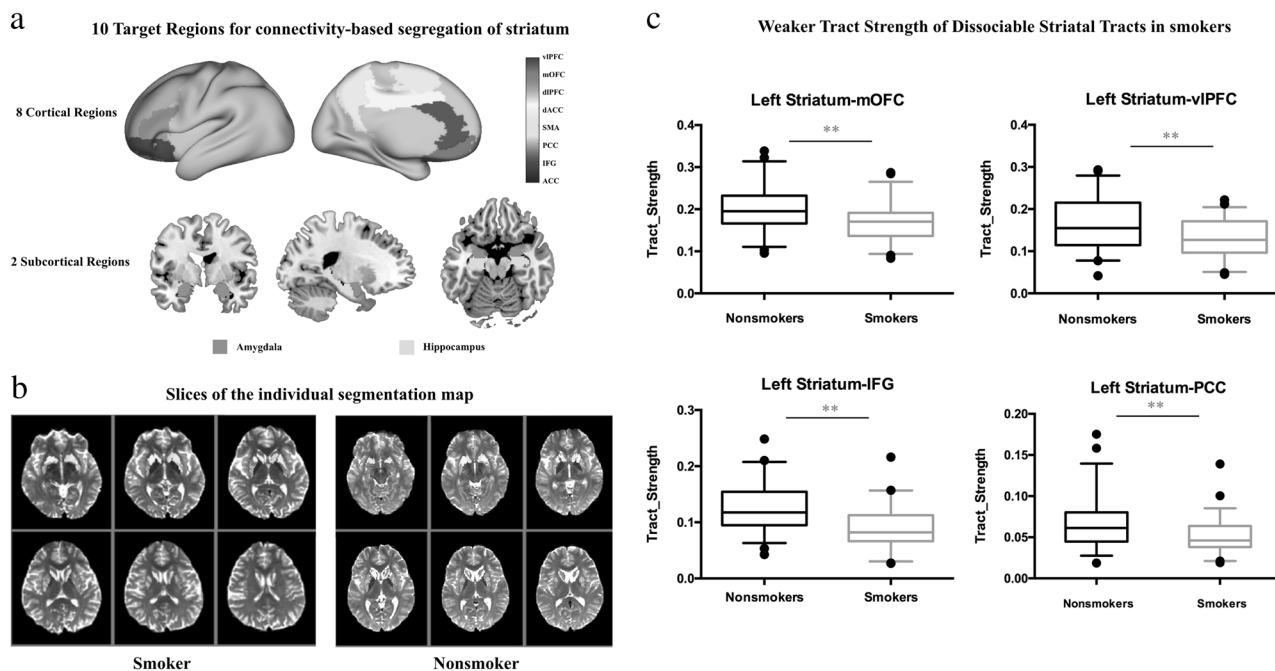
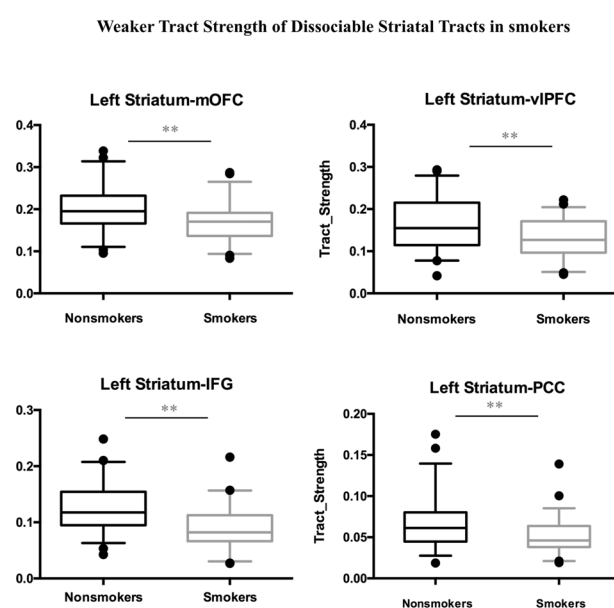


Fig. 1 Target regions for seed-based tractography and different tract strengths of striatal tracts between smokers and nonsmokers. **a** The target brain masks (8 cortical cortex and 2 subcortical regions) for striatum tractography. **b** Slices of the individual segmentation map of striatum (color theme: red–yellow in FSL 5.0.9). **c** The tract strength of striatal tracts was different between smokers and nonsmokers (** $p < 0.0025$, Bonferroni correction)

10 target regions) were transferred to native diffusion space as we described in our previous studies [5, 23].

Probabilistic tractography. DTI spike artifacts were assessed by visual inspection of images by two radiologists who did not identify images with DTI spike artifacts and thus no subject was removed. Preprocessing of DTI data including brain extraction, unwarping of B0 inhomogeneity distortion, correction of eddy current distortion and motion, tensor calculation and fractional anisotropy (FA) maps were conducted using DTI_PREPROCESS, a bash-script wrapper for FSL (https://github.com/RIKEN-BCIL/dti_preprocess). Probabilistic tractography was performed in FSL 5.0.9 (<https://www.fmrib.ox.ac.uk/fsl>) in individual diffusion space. By employing the FDT toolbox, a partial volume mode was used to perform probabilistic tractography, which allowed for up to two fiber directions in each voxel and accounted for crossing fibers [12, 22]. In each voxel in the seed mask (striatum), 5000 sample tracts were generated. Tractography was performed separately for the left and right striatum. We used an exclusion mask of the contralateral hemisphere to restrict the generated tracts to the ipsilateral hemisphere of the seed mask.

Seed-based classification and the tract strength of striatal circuits. Based on standard methodology [12, 22, 24], the voxel values (at least 10 samples) were converted into proportions defined as the number of tracts reaching the target mask for that voxel, divided by the total number of tracts that reach any of the 10 a priori target masks. For each participant, the analyses resulted in 10 value maps in individual diffusion space, one for each target region. Then, the striatum was segmented by assigning each voxel to the region with which it had the highest connection probability (Fig. 1b). For each tract connecting the striatum to 10 a priori masks, the tract strength was calculated as the mean value of the tract probability within each individually determined striatal segment. Finally, for display purposes, each striatal part was then transformed to standard space and overlapped across the majority (defined as 60% here) of subjects.



Statistical analysis
The statistical analyses were conducted using SPSS, version 22 (IBM, Armonk, NY). Independent *t*-tests were used to compare demographic characteristics and tract strength of striatal circuits between smokers and nonsmokers. For the DTI results, Bonferroni corrections were used for multiple comparisons ($p < 0.05/20 = 0.0025$). The correlations between the tract strength and smoking behaviors (i.e., pack-years, FTND, questionnaire of smoking urges, onset, cigarette per day (CPD)) were assessed by Pearson correlations ($p < 0.05/100 = 0.0005$, Bonferroni corrected).

Then, one-way analysis of variance (ANOVA) was used to compare the demographic characteristics and the tract strength of striatal circuits among nonsmokers, abstainers and lapsed smokers ($p < 0.05/20 = 0.0025$). In abstainers, paired *t*-tests were used to assess changes in self-reports of craving, anxiety and depression between the sated and abstinence conditions. Independent *t*-tests were used to compare the smoking behavior variables between abstainers and lapsed smokers.

We employed linear regression analysis to test whether the DTI metrics of striatal circuits were associated with percentage changes in craving in abstainers ($p < 0.05/20 = 0.0025$). In addition, we used a series of binary logistic regression to verify whether and which striatal circuit predicted 12-h abstinence-induced lapse among smokers ($p < 0.05/20 = 0.0025$). The prediction performance of the classification model for lapse was evaluated by 10-fold cross-validation. The whole set of subject samples are equally partitioned into 10 subsets, and then the samples within one subset are selected as the testing dataset and all remaining samples in the other 9 subsets consist of training dataset. This process is repeated for 10 times independently to ensure zero contamination of the training phase of the classifier. Accuracy, sensitivity, specificity, positive predictive value (PPV), negative predictive value (NPV) and area under curve (AUC) of the receiver operating characteristic curve (ROC) were used to quantify our classification performance.

Table 2 Tract strength differences of striatal circuits between smokers and nonsmokers ($p < 0.0025$ Bonferroni correction)

Items	Nonsmokers <i>n</i> = 58	Smokers <i>n</i> = 53	<i>t</i>	<i>P</i> value
Left hemisphere				
vIPFC	0.161 ± 0.060	0.128 ± 0.047	3.17	0.002
mOFC	0.199 ± 0.153	0.169 ± 0.047	3.18	0.002
dIPFC	0.114 ± 0.055	0.100 ± 0.036	1.64 ^a	0.11
dACC	0.037 ± 0.014	0.035 ± 0.013	0.86	0.39
SMA	0.105 ± 0.044	0.099 ± 0.046	0.66	0.51
PCC	0.067 ± 0.031	0.051 ± 0.022	3.24 ^a	0.002
IFG	0.125 ± 0.042	0.090 ± 0.035	4.68	<0.001
ACC	0.038 ± 0.016	0.035 ± 0.019	0.72	0.47
Amygdala	0.122 ± 0.043	0.138 ± 0.047	-1.85	0.07
Hippocampus	0.098 ± 0.033	0.095 ± 0.032	0.39	0.70
Right hemisphere				
vIPFC	0.157 ± 0.054	0.143 ± 0.055	-1.37	0.17
mOFC	0.162 ± 0.049	0.146 ± 0.056	1.65	0.10
dIPFC	0.098 ± 0.033	0.093 ± 0.037	0.77	0.44
dACC	0.070 ± 0.038	0.070 ± 0.031	-0.03	0.98
SMA	0.068 ± 0.033	0.083 ± 0.047	-1.96 ^a	0.053
PCC	0.062 ± 0.023	0.079 ± 0.036	-3.02 ^a	0.003
IFG	0.090 ± 0.026	0.084 ± 0.034	1.14	0.26
ACC	0.035 ± 0.019	0.035 ± 0.015	0.16	0.87
Amygdala	0.085 ± 0.032	0.088 ± 0.033	-0.53	0.60
Hippocampus	0.041 ± 0.019	0.047 ± 0.022	-1.48	0.006

^aNot equal variance
Bold values indicate a statistically significant difference with a *p*-value less than 0.0025 (Bonferroni correction)

RESULTS

There were no differences for age and education between smokers and nonsmokers ($p > 0.05$) (Table 1). However, smokers (satiated condition) showed significantly greater scores in self-reports of anxiety ($t = 2.98$, $p = 0.004$) and depression ($t = 2.29$, $p = 0.024$) than nonsmokers (Table 1).

The tract strength differences between smokers and nonsmokers For quality control of motion in DTI images, we calculated frame-wise displacement and one-way ANOVA analysis demonstrated that there were no significant differences in motion ($F(2, 108) = 0.8$, $p = 0.45$) between lapsed (mean ± SD: 0.25 ± 0.02 mm), abstainers (0.28 ± 0.02 mm) and nonsmokers (0.27 ± 0.01 mm).

After correcting for multiple comparisons ($p < 0.05/20 = 0.0025$), in the left hemisphere, striatum-mOFC ($t = 3.18$, $df = 109$, $p = 0.002$), striatum-vIPFC ($t = 3.17$, $df = 109$, $p = 0.002$), striatum-IFG ($t = 4.68$, $df = 109$, $p < 0.0001$) and striatum-PCC ($t = 3.55$, $df = 109$, $p = 0.002$) showed weaker tract strength in smokers compared with nonsmokers (Fig. 1c and Table 2). No other tracts showed significant group differences ($p < 0.0025$) (Table 2 and Figure S1, S2 in Supplemental Information). Covarying by age, education, anxiety and depression led to similar results with significant group differences in left striatum-mOFC ($t = 11.16$, $df = 105$, $p = 0.001$), striatum-vIPFC ($t = 13.66$, $df = 105$, $p < 0.001$) and striatum-IFG ($t = 24.55$, $df = 105$, $p < 0.0001$) except that the left striatum-PCC ($t = 9.05$, $df = 105$, $p = 0.003$) did not survive correction for multiple comparisons.

Correlation analysis in the smokers between tract strength and smoking behaviors (i.e., pack-years, FTND, craving, CO concentration) did not reveal any significant associations.

Consistent with previous findings [12, 22, 25], the results of the segregations of the left striatum with mOFC, dIPFC, vIPFC and IFG in MNI (Montreal Neurological Institute) space clearly showed that the striatal subregions were connected in specific spatial patterns: NAc with mOFC, caudate with dIPFC, anterior putamen with vIPFC and posterior putamen with IFG (Fig. 2a).

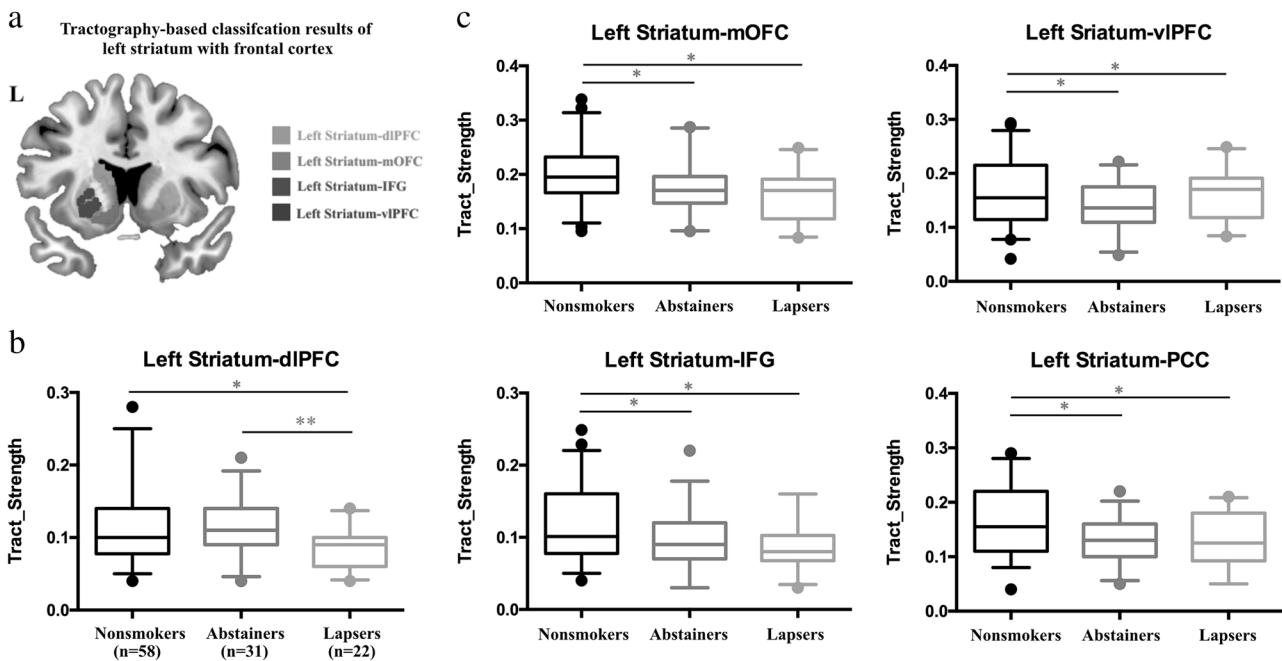


Fig. 2 Tractography-based classification results and the tract strength comparisons among nonsmokers, abstainers and lapsers. **a** Tractography-based classification results of left striatum with frontal cortex (dorsolateral prefrontal cortex (dIPFC), medial orbitofrontal cortex (mOFC), inferior frontal gyrus (IFG), ventral lateral PFC (vIPFC)) in smokers. For display purposes, each striatal part was then transformed to standard MNI (Montreal Neurological Institute) space and overlapped across the majority of subjects (defined as 60% here). **b** The tract strength comparisons of left striatum-dIPFC among the three groups. **c** The tract strength comparisons of left striatum with mOFC, vIPFC, IFG and posterior cingulate cortex (PCC) among the three groups (* $p < 0.05$ uncorrected, ** $p < 0.0025$, Bonferroni correction)

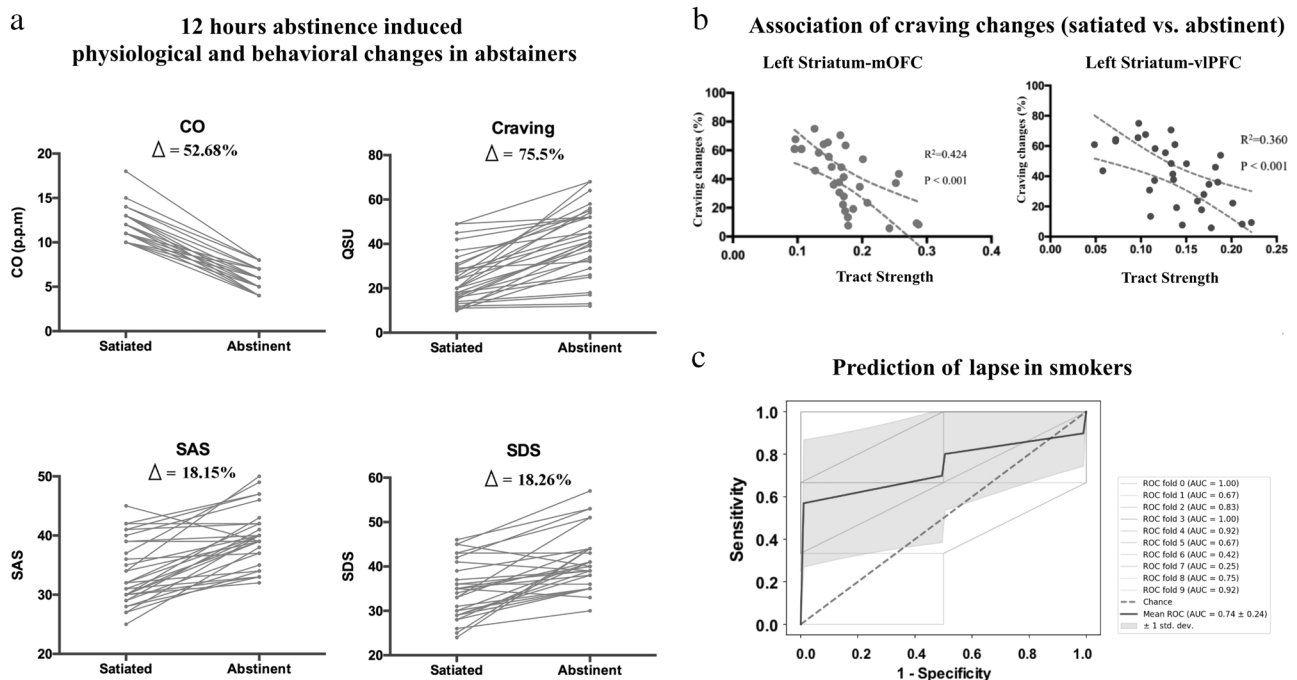


Fig. 3 The 12-h abstinence-induced physiological and behavioral changes and association with striatum tracts. **a** The 12-h abstinence-induced physiological and behavioral changes in 31 abstainers. **b** The tract strength of the left striatum-mOFC and left striatum-vlPFC predicted the 12-h abstinence-induced percent changes in craving. **c** The receiver operating characteristic (ROC) curve for the prediction of 12-h abstinence-induced lapse by the tract strength of left striatum-dlPFC in smokers. dlPFC dorsolateral prefrontal cortex, mOFC medial orbitofrontal cortex, vlPFC ventral lateral PFC

Tract strength of striatal circuits between abstainers, lapsers and nonsmokers

Among 53 smokers, 31 abstainers accomplished the 12-h abstinence procedure. The other 22 lapsers did not return and their failures to keep abstinent were verified by phone calls. The smoking variables were not significantly different between abstainers and lapsers (Table S1 in Supplemental Information). One-way ANOVA of the imaging data revealed the main effects of group were significant for left striatum-IFG ($F(2, 108) = 10.98, p < 0.001$) (Table S2 in Supplemental Information). The results of the left striatum-dlPFC ($F(2, 108) = 4.13, p = 0.02$), left striatum-mOFC ($F(2, 108) = 5.74, p = 0.004$), left striatum-PCC ($F(2, 108) = 5.25, p = 0.007$) and left striatum-vlPFC ($F(2, 108) = 5.00, p = 0.008$) did not survive Bonferroni correction. Post-hoc analysis demonstrated that the tract strength of the left striatum-IFG was weaker in abstainers ($t = 3.6, p < 0.001$) and lapsers ($t = 3.8, p < 0.001$) compared with nonsmokers (Fig. 2c). The tract strength of the left striatum-dlPFC was weaker in lapsers compared with abstainers ($t = 3.28, p = 0.002$, corrected) (Fig. 2b).

Prediction of lapsers by striatal tract strength

In 31 abstainers, craving was significantly increased in the 12-h abstinence condition (41.61 ± 15.27) compared with the satiated condition (23.71 ± 11.41) ($t = 8.40, df = 30, p < 0.0001$) (Fig. 3a). The anxiety ($t = 6.94, df = 30, p < 0.0001$) and depression ($t = 5.81, df = 30, p < 0.0001$) ratings were also higher in the abstinence condition compared with the satiated condition (Fig. 3a). The tract strength of the left striatum-mOFC ($R^2 = 0.424, F = 21.35, p < 0.001$) and left striatum-vlPFC ($R^2 = 0.360, F = 16.56, p < 0.001$) were associated with percentage changes in craving between the satiated and abstinence condition (Fig 3b). In the whole cohort of smokers, the tract strength of the left striatum-dlPFC predicted lapsers (forward: likelihood ratio, $\chi^2 = 11.08, df = 1, p = 0.001$). For the 10-fold cross-validation analysis, the accuracy, sensitivity, specificity, PPV and NPV of this classification model were 68.3, 56.7, 85.0, 75.0 and 59.0%, respectively. The average AUC was 0.74

(Fig. 3c). No other striatal tracts were associated with craving changes or predicted lapsers in smokers. None of the tracts predicted changes in anxiety or depression following 12-h abstinence in smokers.

DISCUSSION

Using a fully automated probabilistic tractography algorithm, we provided a comprehensive description of different striatal tracts based on the connections between striatal seeds and 10 bilateral target regions in 53 smokers and 58 nonsmokers (Fig. 1a, b). In smokers, the left striatum showed weaker tract strength with the left vlPFC, mOFC, IFG and PCC (Fig. 1c). Relative to the satiated condition, the 12-h abstinence procedure induced significant increases in smoking craving, anxiety and depression in 31 abstainers (Fig. 3a). The increases in craving (percent change) were associated with the tract strength of the left striatum-mOFC and left striatum-vlPFC (Fig. 3b). Moreover, among the whole cohort of smokers, the tract strength of the left striatum-dlPFC predicted lapsers with an accuracy of 68.3% (Fig. 3c). Thus, our results provide system-level insights into the abnormal connectivity strength of striatal circuits in smokers and their potential roles as neuroimaging biomarkers for craving changes and to predict risk of lapse.

Consistent with the neuropsychiatric changes of frontostriatal circuits in addiction including smoking [3–5, 8, 10, 16], the majority of findings were related to striato-PFC connections (Figs. 2, 3). The involvement of the mOFC and vlPFC in smoking craving has been demonstrated in previous studies [26, 27]. The mOFC has extensive connections with the striatum and limbic regions [28]. The activation of the mOFC [29, 30] and vlPFC [31] was associated with smoking cue-induced craving in smokers. In an arterial spin labeling MRI study, abstinence-induced smoking craving was predicted by cerebral blood flow increases (abstinence minus satiated) in the mOFC and NAc [29]. The vlPFC has been strongly associated with impulsive and compulsive

drug-seeking behaviors [32] and with craving in addiction [33, 34]. Dysfunction of vIPFC may contribute to attention bias toward drug-related stimuli and away from other stimuli to procure the drug [32]. Indeed, the interactions of striatum with vIPFC and mOFC for craving regulation had also been detected by Kober et al. [10], where smokers recruited vIPFC and mOFC during cognitive effort to reduce smoking craving by down-regulating the activation of ventral striatum. Previous studies demonstrated that the function of striatal circuits is regulated by their anatomical connectivity patterns [12, 22]. Thus, the present findings of weaker tract strength of left striatum-mOFC and left striatum-vIPFC in smokers fit well with the functional findings mentioned above.

To explore the clinical implications of DTI results, we also assessed their potential roles to predict lapsers. We found that the tract strength of the left striatum-dIPFC predicted lapsers induced by 12-h abstinence in smokers with 68.3% accuracy. We previously observed that the weaker resting-state functional connectivity of dorsal striatum-dIPFC circuit correlated with impaired Stroop task performances in smokers [4]. Cognitive control has been shown to be regulated by striatum-dIPFC tracts [11, 35], and its developmental improvements are paralleled by increases in activation and functional connectivity of the striatum-dIPFC circuit [36]. The coherence of the striatum-dIPFC circuit could account for individual differences in cognitive control in healthy subjects [11, 35] and in addicted users [37–39]. Thus, our results of left striatum-dIPFC tract strength predicting lapsers may relate to individual differences in cognitive control, which was consistent with a recent study showing that baseline differences in cognitive control could predict smoking relapse [40]. In sum, we report a potential novel WM biomarker to predict 12 h abstinence-induced lapse in smokers.

We also observed that the left striatum-IFG and the left striatum-PCC showed weaker tract strength in smokers relative to nonsmokers (Fig. 1c). The left IFG plays a role in inhibitory processes [41] and has been implicated in top-down control over craving in addiction [32]. In treatment-seeking cigarette smokers, the instruction to resist craving while viewing smoking-related videos was associated with IFG activation, which was positively correlated with craving [42]. Cognitive regulation strategies enhanced activation of the IFG to suppress craving in smokers [10]. In addition, the PCC has been implicated in memory retrieval, attention tracking of stimuli and in the preparation of motor behaviors directed at these stimuli [26, 42]. The large and consistent activation of PCC was detected in smoking cue reactivity tasks in smokers [26], which might reflect smokers' attention bias toward the smoking cues, or preparing for the physical act of smoking in response to these stimuli. However, more work is needed to explicitly link weaker tract strength in these regions with impaired inhibitory control and attention bias in the future.

The predominant left lateralization of the findings in the current study is consistent with previous DTI [13] and striatal morphology [43] studies in smokers. Zhang et al. [44] recently demonstrated that the left ventral striatum may be more important than the right striatum in linking saliency response to internal process. The striatum and the PFC are mainly modulated via cortico-striatal DA and glutamatergic circuits [16]. Cortical regulation of DA transmission in the NAc appears to be stronger in the left hemisphere [45]. In support, theta burst magnetic brain stimulation of the left but not right hemispheric dIPFC inhibited DA release bilaterally in the caudate and unilaterally in the putamen [46].

Of note, previous studies have reported inconsistent WM findings in smokers [14, 47]. Differences in the age of participants (young vs. adult) and data analysis methods (tract-based spatial statistics vs. DTI tractography) might explain some of the

discrepancies between studies. In particular, a better understanding of the relationship between reduced tract strength and abnormal FA might help clarify the different results obtained with these methodologies in smokers.

Limitations

Our results may only generalize to males, since gender differences related to smoking have been observed [48, 49]. The cross-sectional nature of this study cannot separate cause from effect for smoking and DTI findings in the present study. Longitudinal studies started before the initiation of smoking will be necessary to address these questions. In addition, the method used for registering the FA maps to the structural scans might have biased our results and replication of our results in a larger sample and utilizing the B0 images is needed. Further, although we instructed participants to have a good night's sleep, we did not collect information on sleep duration, quality, and diurnal patterns before the study days. Therefore, our neuroimaging findings may have been confounded by differences in sleep quality and the time of awakening. Also, an accuracy of 68.3% is only moderate and this methodology will need to be refined to improve accuracy before being of utility for clinical purposes. Finally, although we focused on fronto-striatal connections here, the insula is a cortical region closely associated with smoking [50], and it will be an intriguing target for future DTI studies.

CONCLUSION

Weaker tract strengths of left striatal circuits with PFC regions (i.e., mOFC, vIPFC and IFG) and with PCC were detected in young male smokers relative to nonsmokers. The tract strength of left striatum-vIPFC, left striatum-mOFC and left striatum-dIPFC might have potential as neuroimaging biomarkers for abstinence-induced craving and to predict lapsers. Strategies to enhance tract strength of specific striato-cortical tracts could help ease craving and prevent lapse in smokers.

ACKNOWLEDGEMENTS

FUNDING

This work is supported by the National Natural Science Foundation of China under Grant Nos. 81871426, 81871430, 81571751, 81571753, 61771266, 31800926 and 81701780, the Fundamental Research Funds for the Central Universities under the Grant No. JB151204, the program for Young Talents of Science and Technology in Universities of Inner Mongolia Autonomous Region NJYT-17-B11, the Natural Science Foundation of Inner Mongolia under Grant No. 2017MS(LH) 0814, the program of Science and Technology in Universities of Inner Mongolia Autonomous Region NJZY17262, the Innovation Fund Project of Inner Mongolia University of Science and Technology No. 2015QNGG03, National Natural Science Foundation of Shaanxi Province under Grant no. 2018JM7075 and the US National Institutes of Health, Intramural Research program Y1AA3009. We thank Zaixu Cui from University of Pennsylvania for his technical assistance in prediction methods.

ADDITIONAL INFORMATION

Supplementary Information accompanies this paper at (<https://doi.org/10.1038/s41386-018-0182-x>).

Competing interests: The authors declare no competing interests.

Ethics statement: The study was approved by the ethics committee of medical research in First Affiliated Hospital of Baotou Medical College, Inner Mongolia University of Science and Technology, Baotou, China. After the study procedure was fully explained, all participants gave written informed consent. All experimental procedures followed the guidelines of human medical research (Declaration of Helsinki).

Publisher's note: Springer Nature remains neutral with regard to jurisdictional claims in published maps and institutional affiliations.

REFERENCES

1. Barrett SP, Boileau I, Okker J, Pihl RO, Dagher A. The hedonic response to cigarette smoking is proportional to dopamine release in the human striatum as measured by positron emission tomography and [¹¹C] raclopride. *Synapse*. 2004;54:65–71.
2. Brody AL, Olmstead RE, London ED, Farahi J, Meyer JH, Grossman P, et al. Smoking-induced ventral striatum dopamine release. *Am J Psychiatry*. 2004;161:1211–8.
3. Volkow ND, Wang G-J, Fowler JS, Tomasi D, Telang F. Addiction: beyond dopamine reward circuitry. *Proc Natl Acad Sci USA*. 2011;108:15037–42.
4. Yuan K, Yu D, Bi Y, Li Y, Guan Y, Liu J, et al. The implication of frontostriatal circuits in young smokers: a resting-state study. *Hum Brain Mapp*. 2016;37:2013–16.
5. Yuan K, Yu D, Bi Y, Wang R, Li M, Zhang Y, et al. The left dorsolateral prefrontal cortex and caudate pathway: new evidence for cue-induced craving of smokers. *Hum Brain Mapp*. 2017;38:4644–56.
6. Galván A, Poldrack RA, Baker CM, McClennen KM, London ED. Neural correlates of response inhibition and cigarette smoking in late adolescence. *Neuropsychopharmacology*. 2011;36:970–8.
7. Ghahremani DG, Faulkner P, Cox C, London ED. Behavioral and neural markers of cigarette-craving regulation in young-adult smokers during abstinence and after smoking. *Neuropsychopharmacology*. 2018;43:1616.
8. Volkow ND, Morales M. The brain on drugs: from reward to addiction. *Cell*. 2015;162:712–25.
9. Sutherland MT, McHugh MJ, Pariyadath V, Stein EA. Resting state functional connectivity in addiction: lessons learned and a road ahead. *Neuroimage*. 2012;62:2281–95.
10. Kober H, Mende-Siedlecki P, Kross EF, Weber J, Mischel W, Hart CL, et al. Prefrontal–striatal pathway underlies cognitive regulation of craving. *Proc Natl Acad Sci USA*. 2010;107:14811–6.
11. Liston C, Watts R, Tottenham N, Davidson MC, Niogi S, Ulug AM, et al. Frontostriatal microstructure modulates efficient recruitment of cognitive control. *Cereb Cortex*. 2006;16:553–60.
12. Van den Bos W, Rodriguez CA, Schweitzer JB, McClure SM. Adolescent impatience decreases with increased frontostriatal connectivity. *Proc Natl Acad Sci USA*. 2015;112:3765–74.
13. Savjani RR, Velasquez KM, Thompson-Lake DGY, Baldwin PR, Eagleman DM, De La Garza R II, et al. Characterizing white matter changes in cigarette smokers via diffusion tensor imaging. *Drug Alcohol Depend*. 2014;145:134–42.
14. Yu D, Yuan K, Zhang B, Liu J, Dong M, Jin C, et al. White matter integrity in young smokers: a tract-based spatial statistics study. *Addict Biol*. 2016;21:679–87.
15. Zhang Y, Li M, Wang R, Bi Y, Li Y, Yi Z, et al. Abnormal brain white matter network in young smokers: a graph theory analysis study. *Brain Imaging Behav*. 2018;12:345–56.
16. Volkow ND, Koob GF, McLellan AT. Neurobiologic advances from the brain disease model of addiction. *New Engl J Med*. 2016;374:363–71.
17. Zelle SL, Gates KM, Fiez JA, Sayette MA, Wilson SJ. The first day is always the hardest: functional connectivity during cue exposure and the ability to resist smoking in the initial hours of a quit attempt. *Neuroimage*. 2017; 151:24–32.
18. Kenford SL, Fiore MC, Jorenby DE, Smith SS, Wetter D, Baker TB. Predicting smoking cessation: who will quit with and without the nicotine patch. *JAMA*. 1994;271:589–94.
19. Owens MM, MacKillop J, Gray JC, Hawkshead BE, Murphy CM, Sweet LH. Neural correlates of graphic cigarette warning labels predict smoking cessation relapse. *Psychiatry Res Neuroimaging*. 2017;262:63–70.
20. Sweitzer MM, Geier CF, Addicott MA, Denlinger R, Raiff BR, Dallery J, et al. Smoking abstinence-induced changes in resting state functional connectivity with ventral striatum predict lapse during a quit attempt. *Neuropsychopharmacology*. 2016;41:2521.
21. Versace F, Engelmann JM, Robinson JD, Jackson EF, Green CE, Lam CY, et al. Prequit fMRI responses to pleasant cues and cigarette-related cues predict smoking cessation outcome. *Nicotine Tob Res*. 2013;16:697–708.
22. van den Bos W, Rodriguez CA, Schweitzer JB, McClure SM. Connectivity strength of dissociable striatal tracts predict individual differences in temporal discounting. *J Neurosci*. 2014;34:10298–10.
23. Yuan K, Qin W, Yu D, Bi Y, Xing L, Jin C, et al. Core brain networks interactions and cognitive control in internet gaming disorder individuals in late adolescence/early adulthood. *Brain Struct Funct*. 2016;221:1427–42.
24. Cohen MX, Schoene-Bake J-C, Elger CE, Weber B. Connectivity-based segregation of the human striatum predicts personality characteristics. *Nat Neurosci*. 2009;12:32.
25. Leh SE, Pfito A, Chakravarty MM, Strafella AP. Fronto-striatal connections in the human brain: a probabilistic diffusion tractography study. *Neurosci Lett*. 2007;419:113–8.
26. Engelmann JM, Versace F, Robinson JD, Minnix JA, Lam CY, Cui Y, et al. Neural substrates of smoking cue reactivity: a meta-analysis of fMRI studies. *Neuroimage*. 2012;60:252–62.
27. Brody AL, Mandelkern MA, London ED, Childress AR, Lee GS, Bota RG, et al. Brain metabolic changes during cigarette craving. *Arch Gen Psychiatry*. 2002;59:1162–72.
28. Groenewegen HJ, Uylings HB. The prefrontal cortex and the integration of sensory, limbic and autonomic information. *Prog Brain Res*. 2000;126:3–28.
29. Wang Z, Faith M, Patterson F, Tang K, Kerrin K, Wileyto EP, et al. Neural substrates of abstinence-induced cigarette cravings in chronic smokers. *J Neurosci*. 2007;27:14035–40.
30. David SP, Munafò MR, Johansen-Berg H, Smith SM, Rogers RD, Matthews PM, et al. Ventral striatum/nucleus accumbens activation to smoking-related pictorial cues in smokers and nonsmokers: a functional magnetic resonance imaging study. *Biol Psychiatry*. 2005;58:488–94.
31. Goudriaan AE, De Ruiter MB, Van Den Brink W, Oosterlaan J, Veltman DJ. Brain activation patterns associated with cue reactivity and craving in abstinent problem gamblers, heavy smokers and healthy controls: an fMRI study. *Addict Biol*. 2010;15:491–503.
32. Goldstein RZ, Volkow ND. Dysfunction of the prefrontal cortex in addiction: neuroimaging findings and clinical implications. *Nat Rev Neurosci*. 2011;12:652–69.
33. Volkow ND, Fowler JS, Wang G-J, Telang F, Logan J, Jayne M, et al. Cognitive control of drug craving inhibits brain reward regions in cocaine abusers. *Neuroimage*. 2010;49:2536–43.
34. Volkow ND, Wang G-J, Ma Y, Fowler JS, Wong C, Ding Y-S, et al. Activation of orbital and medial prefrontal cortex by methylphenidate in cocaine-addicted subjects but not in controls: relevance to addiction. *J Neurosci*. 2005;25:3932–9.
35. Casey B, Epstein J, Buhle J, Liston C, Davidson M, Tonev S, et al. Fronto-striatal connectivity and its role in cognitive control in parent-child dyads with ADHD. *Am J Psychiatry*. 2007;164:1729–36.
36. Vink M, Zandbelt BB, Gladwin T, Hillegers M, Hoogendam JM, den Wildenberg WP, et al. Fronto-striatal activity and connectivity increase during proactive inhibition across adolescence and early adulthood. *Hum Brain Mapp*. 2014;35:4415–27.
37. Hanlon CA, Wesley MJ, Stapleton JR, Laurienti PJ, Porrino LJ. The association between frontal–striatal connectivity and sensorimotor control in cocaine users. *Drug Alcohol Depend*. 2011;115:240–3.
38. Morein-Zamir S, Robbins TW. Fronto-striatal circuits in response-inhibition: relevance to addiction. *Brain Res*. 2015;1628:117–29.
39. Yuan K, Yu D, Cai C, Feng D, Li Y, Bi Y, et al. Fronto-striatal circuits, resting state functional connectivity and cognitive control in internet gaming disorder. *Addict Biol*. 2017;22:813–22.
40. Froeliger B, McConnell PA, Bell S, Sweitzer M, Kozink RV, Eichberg C, et al. Association between baseline corticothalamic-mediated inhibitory control and smoking relapse vulnerability. *JAMA Psychiatry*. 2017;74:379–86.
41. Swick D, Ashley V, Turken U. Left inferior frontal gyrus is critical for response inhibition. *BMC Neurosci*. 2008;9:102.
42. Brody AL, Mandelkern MA, Olmstead RE, Jou J, Tjongson E, Allen V, et al. Neural substrates of resisting craving during cigarette cue exposure. *Biol Psychiatry*. 2007;62:642–51.
43. Janes AC, Park MTM, Farmer S, Chakravarty MM. Striatal morphology is associated with tobacco cigarette craving. *Neuropsychopharmacology*. 2015;40:406–11.
44. Zhang S, Hu S, Chao HH, Chiang-shan RL. Hemispheric lateralization of resting-state functional connectivity of the ventral striatum: an exploratory study. *Brain Struct Funct*. 2017;222:2573–83.
45. Louilot A, Le Moal M. Lateralized interdependence between limbic-temporal and ventrostriatal dopaminergic transmission. *Neuroscience*. 1994;59:495–500.
46. Ko JH, Monchi O, Pfito A, Bloomfield P, Houle S, Strafella AP. Theta burst stimulation-induced inhibition of dorsolateral prefrontal cortex reveals hemispheric asymmetry in striatal dopamine release during a set-shifting task—a TMS-[¹¹C] raclopride PET study. *Eur J Neurosci*. 2008;28:2147–55.
47. Huang P, Shen Z, Wang C, Qian W, Zhang H, Yang Y, et al. Altered white matter integrity in smokers is associated with smoking cessation outcomes. *Front Hum Neurosci*. 2017;11:438.
48. Brown AK, Mandelkern MA, Farahi J, Robertson C, Ghahremani DG, Sumerel B, et al. Sex differences in striatal dopamine D2/D3 receptor availability in smokers and non-smokers. *Int J Neuropsychopharmacol*. 2012;15:989–94.
49. Cosgrove KP, Wang S, Kim S-J, McGovern E, Nabulsi N, Gao H, et al. Sex differences in the brain's dopamine signature of cigarette smoking. *J Neurosci*. 2014;34:16851–5.
50. Naqvi NH, Rudrauf D, Damasio H, Bechara A. Damage to the insula disrupts addiction to cigarette smoking. *Science*. 2007;315:531–4.